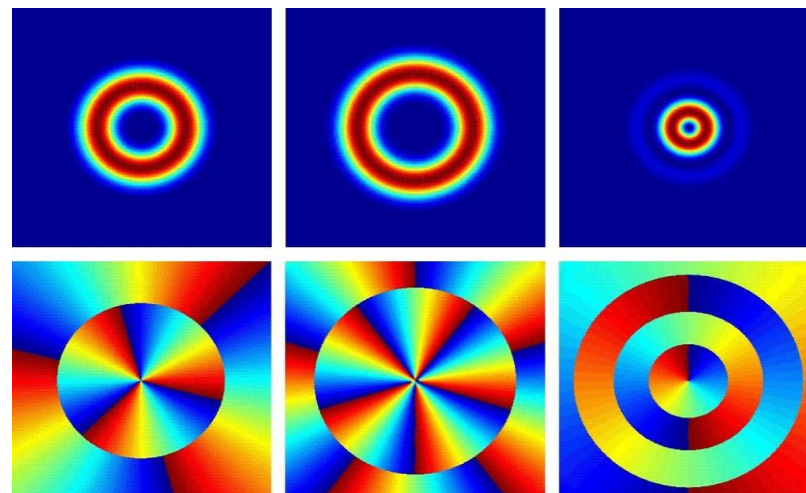


Rezonanse typu spin-orbit w meta-materiałowych elementach nanofotoniki

Spin-orbit resonances in meta-material elements of nanophotonics

Wojciech Nasalski

*Zespół Badawczy Nanofotoniki
Instytut Podstawowych Problemów Techniki
Polskiej Akademii Nauk*



References

Vectorial description of optical 3D beams

1. W. Nasalski, "Three-dimensional beam reflection at dielectric interfaces", Opt. Commun. **197**, 217-233 (2001).
2. W. Nasalski, "Amplitude-polarization representation of three-dimensional beams at a dielectric interface", J. Opt. A: Pure Appl. Opt. **5**, 128-136 (2003).
3. W. Nasalski, *Optical beams at dielectric interfaces - fundamentals*, in Series: Trends in Mechanics of materials (IPPT PAN, Warsaw 2007).

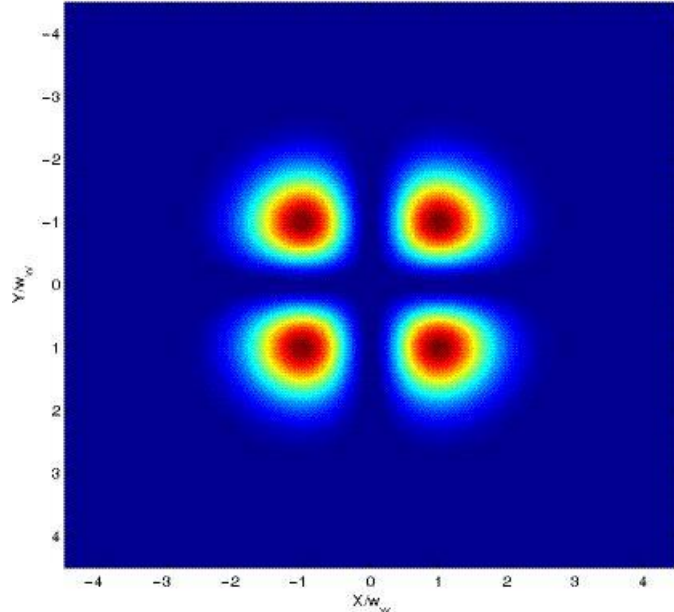
Cross-polarization (XPC) spin-orbit conversion of optical vortices nested in optical beams

4. W. Nasalski, "Polarization versus spatial characteristics of optical beams at a planar isotropic interface", Phys. Rev. E **74**, 056613-1-16 (2006).
5. W. Nasalski and Y. Pagani, "Excitation and cancellation of higher-order beam modes at isotropic interfaces", J. Opt. A: Pure Appl. Opt. **8**, 21-29 (2006).
6. W. Szabelak and W. Nasalski, "Transmission of Elegant Laguerre-Gaussian beams at a dielectric interface - numerical simulations", Bull. Pol. Ac. Tech. **57**, 181-188 (2009).
7. W. Nasalski, "Cross-polarized normal mode patterns at a dielectric interface", Bull. Pol. Ac. Tech. **58**, 141-154 (2010).

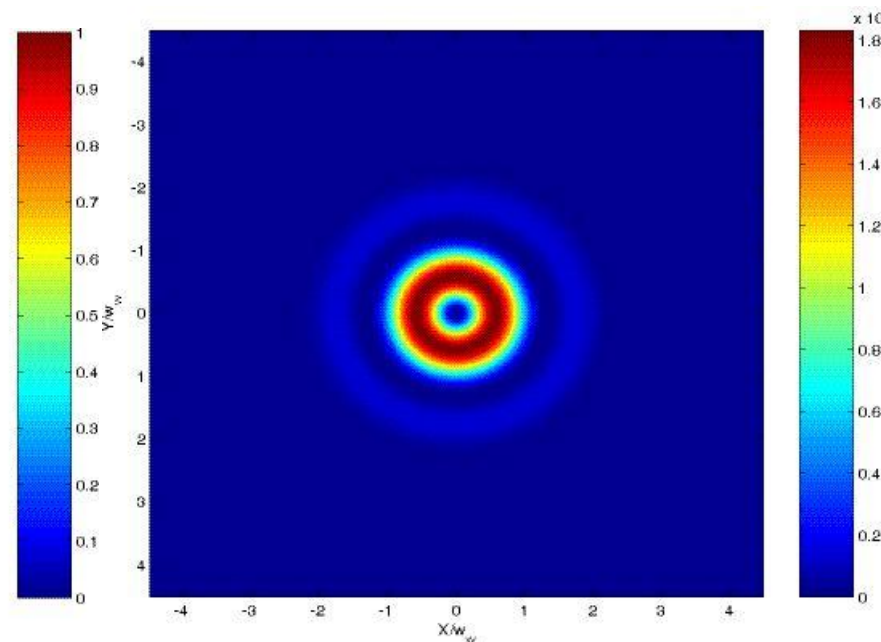
Application of planar and resonant meta-material structures – enhancement of the XPC

8. W. Szabelak and W. Nasalski, "Enhancement of cross-polarized beam components at a metamaterial surface", Appl. Phys. B - Lasers and Optics **103**, 369-375 (2011).
9. W. Szabelak and W. Nasalski, "Cross-polarization coupling and switching in an open nano-meta-resonator", J. Phys. B. At. Mol. Opt. Phys. **44**, 215403 (2011); *featured by Institute of Physics, UK*.

Optical field intensity in the beam transverse plane



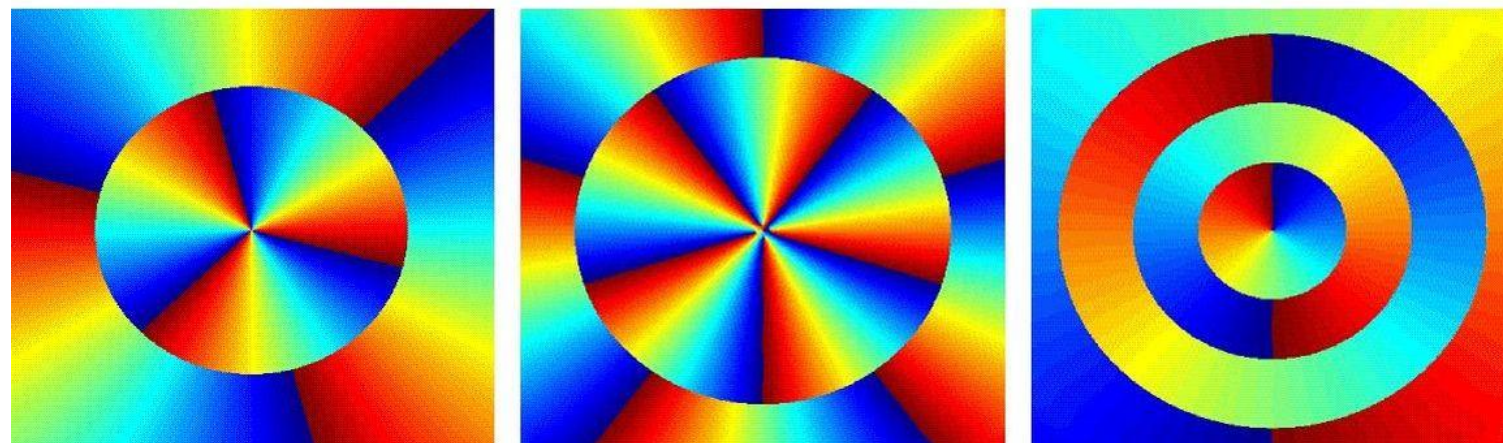
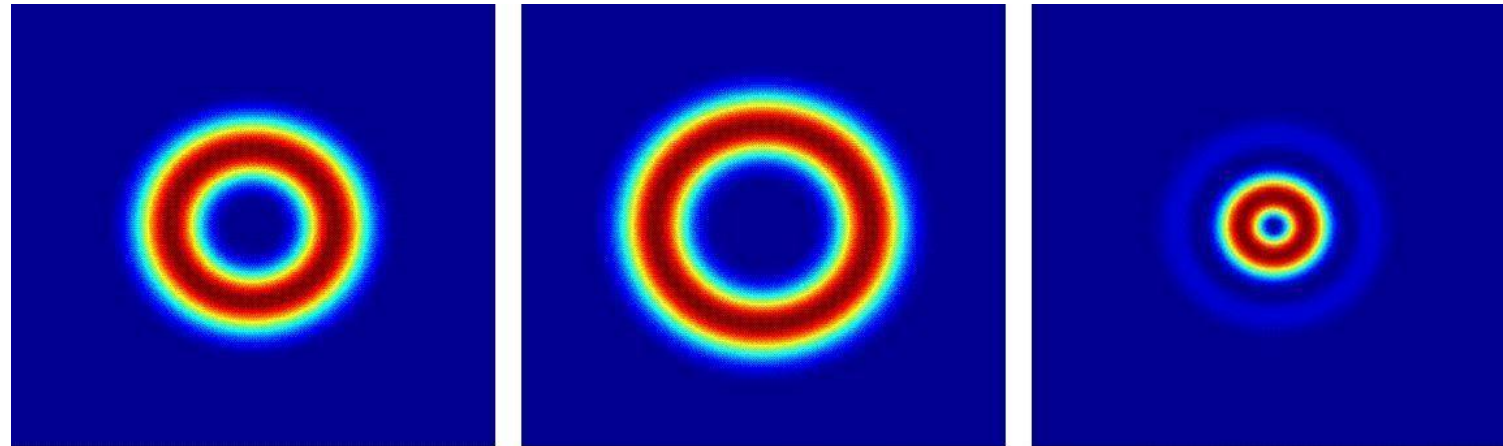
Elegant Hermite-Gaussian beam
EHG_{1,1} pattern
topological charge l = 0
transverse Cartesian symmetry



Elegant Laguerre-Gaussian beam
ELG_{2,1} pattern
topological charge l = 1
transverse cylindrical symmetry

WN, Phys. Rev. E (2006)

Optical field intensity and phase in the beam transverse plane



$\text{ELG}_{1,3}$

topological charge $l = 3$

$\text{ELG}_{0,3}$

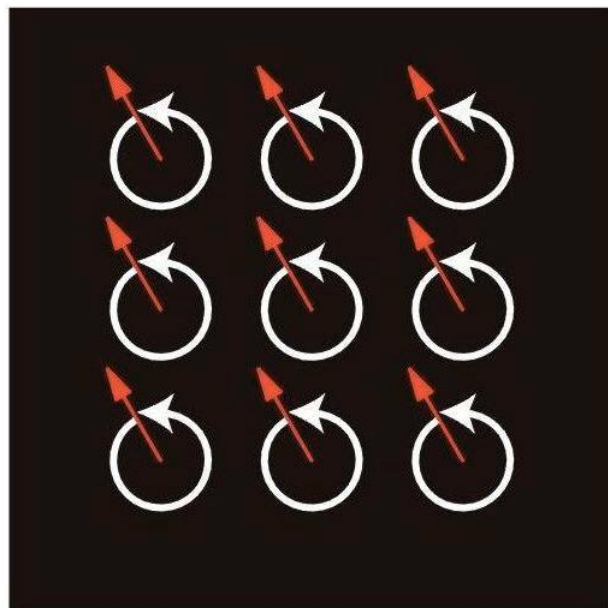
topological charge $l = 5$

$\text{ELG}_{2,1}$

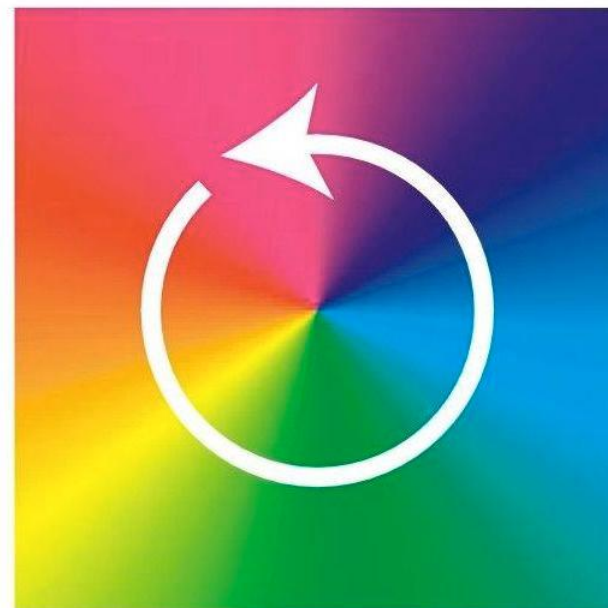
topological charge $l = 1$

WN, Phys. Rev. E (2006)

Optical field polarization and phase in the beam transverse plane



spin



OAM

Rotation of spin (left) and orbital angular momentum (OAM, right) states.

J. Courtial, et al., (2006)

Rada Naukowa IPPT PAN, sesja sprawozdawcza 26.04.2012

Paraxial monochromatic complex argument (“elegant”) beams

Hermite-Gaussian EHG beams in Cartesian coordinates $X - Y - Z$ and polarization frames $|\underline{\underline{X}}\rangle - |\underline{\underline{Y}}\rangle$:

$$\underline{\underline{E}}_{m,n}^{(EH)}(X,Y,Z) = (\alpha|\underline{\underline{X}}\rangle + \beta|\underline{\underline{Y}}\rangle) \quad G_{m,n}^{(EH)}(X,Y,Z) \exp(-i\omega t + ikZ)$$

vector polarization \leftrightarrow scalar spatial distribution plane-wave phase factor

Fock – Schrödinger equation:

$$\left\{ ik \partial_Z + \frac{1}{2} (\partial_X^2 + \partial_Y^2) \right\} G_{m,n}^{(EH)}(X,Y,Z) = 0$$

solutions in terms of Hermite polynomials H_m and Gaussian function $G_{0,0}$ (A.E.Siegman (1973)):

$$G_{m,n}^{(EH)}(X,Y,Z) = (-w_w)^{m+n} H_m(2^{-1/2} X/v(Z)) H_n(2^{-1/2} Y/v(Z)) G_{0,0}^{(EH)}(X,Y,Z)$$

no vortex, topological charge $q = 0$

Laguerre-Gaussian ELG beams in cylindrical coordinates $\rho - \varphi - Z$ and polarization frames $|\underline{\underline{CR}}\rangle - |\underline{\underline{CL}}\rangle$:

$$\underline{\underline{E}}_{p,l}^{(EL)}(r,\psi,Z) = (\alpha|\underline{\underline{CR}}\rangle + \beta|\underline{\underline{CL}}\rangle) G_{p,l}^{(EL)}(\zeta, \bar{\zeta}, Z) \exp(-i\omega t + ikZ)$$

Fock – Schrödinger equation:

$$\left\{ ik \partial_Z + \partial_\zeta \partial_{\bar{\zeta}} \right\} G_{p,l}^{(EL)}(\zeta, \bar{\zeta}, Z') = 0 \quad \zeta, \bar{\zeta} = 2^{-1/2} (X \pm iY) = 2^{-1/2} \varphi \exp(\pm i\varphi)$$

solution in terms of Laguerre polynomials L_p^l and Gaussian function $G_{0,0}$:

$$G_{p,l}^{(EL)}(\zeta, \bar{\zeta}, Z') = (-1)^{p+l} (\zeta_\perp/v)^l (v/w_w)^{-(2p+l)} p! L_p^l(\zeta_\perp^2/v^2) G_{0,0}^{(EL)}(\zeta, \bar{\zeta}, Z) \exp(il\varphi)$$

with vortex, topological charge $q = 1$

WN, Phys. Rev. E (2006); Bull. Pol. Ac.: Tech. (2010)

Rada Naukowa IPPT PAN, sesja sprawozdawcza 26.04.2012

Transmission matrix for beams at dielectric interfaces and multilayers

with (known) Fresnel transmission coefficients t_p of TM ($E \equiv E_x$) and t_s of TE ($E \equiv E_y$) polarization

in Cartesian transverse coordinates $X - Y$ (for HG beams of TM or TE polarization)

$$\text{for plane waves: } \hat{T} = \begin{bmatrix} t_p & 0 \\ 0 & t_s \end{bmatrix}$$

$$\text{for beams: } \hat{T} = \frac{1}{2}(t_p + t_s) \begin{bmatrix} 1 & 0 \\ 0 & 1 \end{bmatrix} + \frac{1}{2}(t_p - t_s) \begin{bmatrix} \cos 2\varphi & \sin 2\varphi \\ \sin 2\varphi & -\cos 2\varphi \end{bmatrix}$$

XPC

in cylindrical transverse coordinates $r - \varphi$ (for LG beams of CR or CL polarization)

$$\text{for plane waves: } \hat{T} = \frac{1}{2} \begin{bmatrix} t_p + t_s & t_p - t_s \\ t_p - t_s & t_p + t_s \end{bmatrix}$$

$$\text{for beams: } \hat{T} = \frac{1}{2}(t_p + t_s) \begin{bmatrix} 1 & 0 \\ 0 & 1 \end{bmatrix} + \frac{1}{2}(t_p - t_s) \begin{bmatrix} 0 & \exp(-2i\varphi) \\ \exp(+2i\varphi) & 0 \end{bmatrix}$$

XPC

non-diagonals $\exp(\pm 2i\varphi)$ induce the spin-orbit XPC conversion leading to vortex excitation or annihilation

for incidence of the CR polarization of ELG beam G_p^l of radial index p and topological charge l

it is excited the CL polarization of ELG beam G_{p-1}^{l+2} of radial index $p-1$ and topological charge $l+2$

for incidence of the CL polarization of ELG beam G_p^l of radial index p and topological charge l

it is excited the CR polarization of ELG beam G_{p+1}^{l-2} of radial index $p+1$ and topological charge $l-2$

thus, the process is controlled by polarization CR or CL of the incident beam

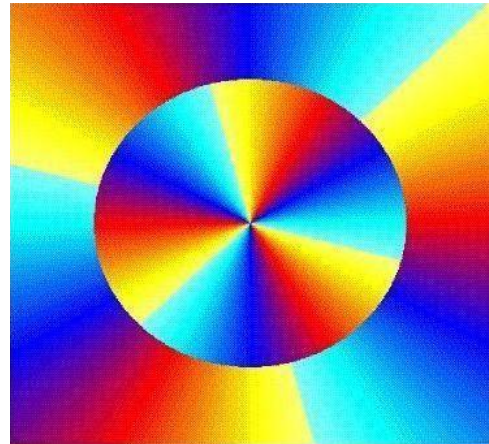
WN, Phys. Rev. E (2006); Bull. Pol. Ac.: Tech. (2010)

Rada Naukowa IPPT PAN, sesja sprawozdawcza 26.04.2012

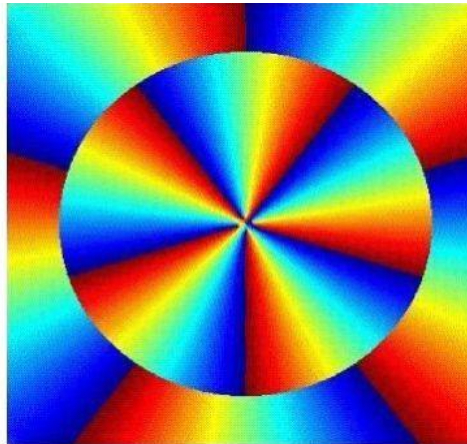
Vortex excitation at a dielectric Interface

first row – circular right-handed (CR) polarization of the incident beam

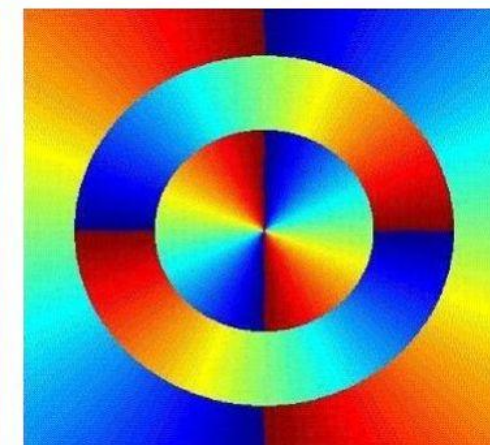
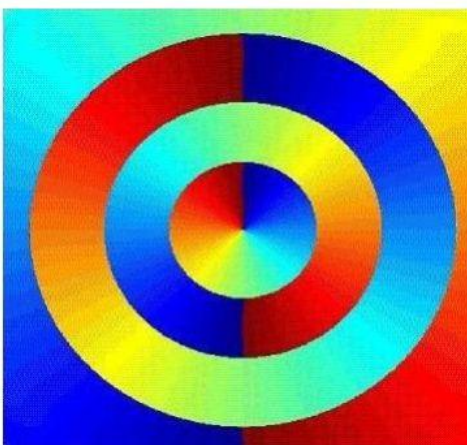
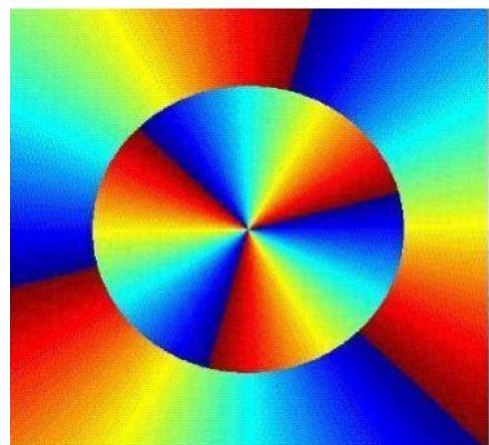
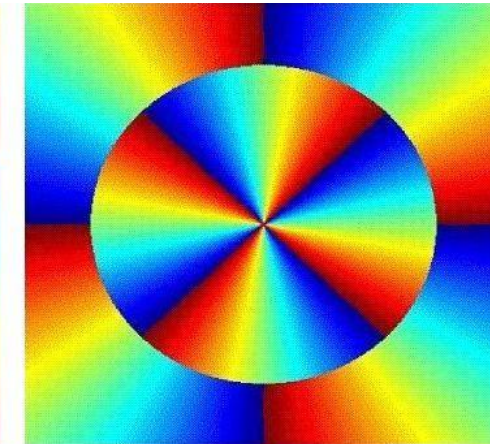
incident CR ELG_{1,3} beam



transmitted CL ELG_{0,5} beam



transmitted Z ELG_{1/2,4} beam



incident CL ELG_{1,3} beam

transmitted CR ELG_{2,1} beam

transmitted Z ELG_{3/2,2} beam

second row – circular left-handed (CL) polarization of the incident beam

Spin-to-orbital angular momentum SAM-to-OAM conversion

SAM is associated with optical polarization and OAM is associated with optical wavefront at conventional (dielectric and transparent) planar interfaces and multilayers

total angular momentum is conserved exactly
for each individual photon in the beam

$$l\hbar = (l_{\text{spin}} + l_{\text{orbital}})\hbar = \text{const.}$$

and for the whole beam field of cylindrical symmetry

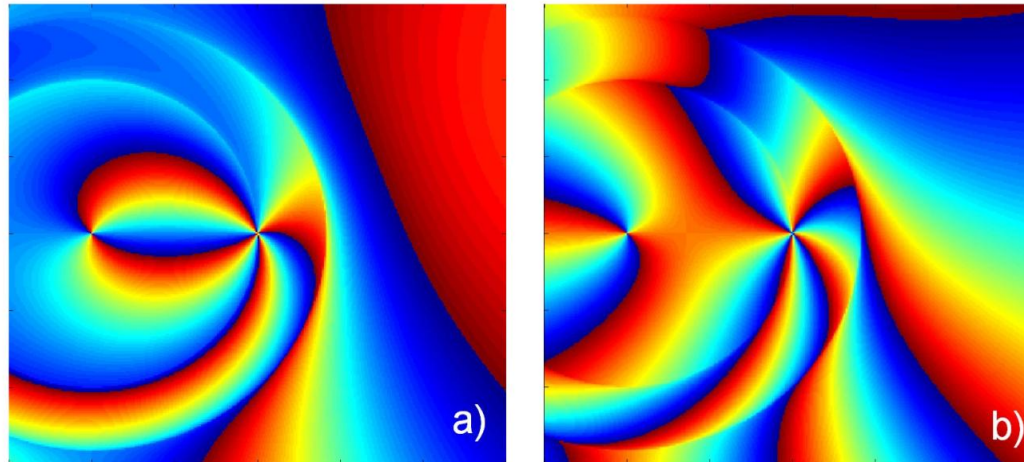
$$L_z = L_{\text{spin}} + L_{\text{orbital}} = \text{const.}$$

what results in
entanglement of spin and orbital parts of beam fields

$$\begin{array}{ccc} \alpha |CR\rangle + \beta |CL\rangle & \Leftrightarrow & \mathbf{ELG}_{p,l}(r, \varphi, z) \\ \text{qubits} & \Leftrightarrow & \text{qudits} \end{array}$$

Vortex excitation and splitting induced by XPC effects at interfaces and multilayers

oblique incident beam of the $\text{ELG}_{2,4}$ shape with $L_{\text{orbit}} = + 4\hbar$



(a) for CL polarization of the incident beam

input: $L_{\text{spin}} = - \hbar$, $L_{\text{orbit}} = + 4\hbar$,

output: $L_{\text{spin}} = + \hbar$, $L_{\text{orbit}} = + 2\hbar$,

$L_z = L_{\text{spin}} + L_{\text{orbit}} = 3\hbar$ per photon

$L_z = L_{\text{spin}} + L_{\text{orbit}} = 3\hbar$ per photon

(b) for CR polarization of the incident beam

input: $L_{\text{spin}} = + \hbar$, $L_{\text{orbit}} = + 4\hbar$,

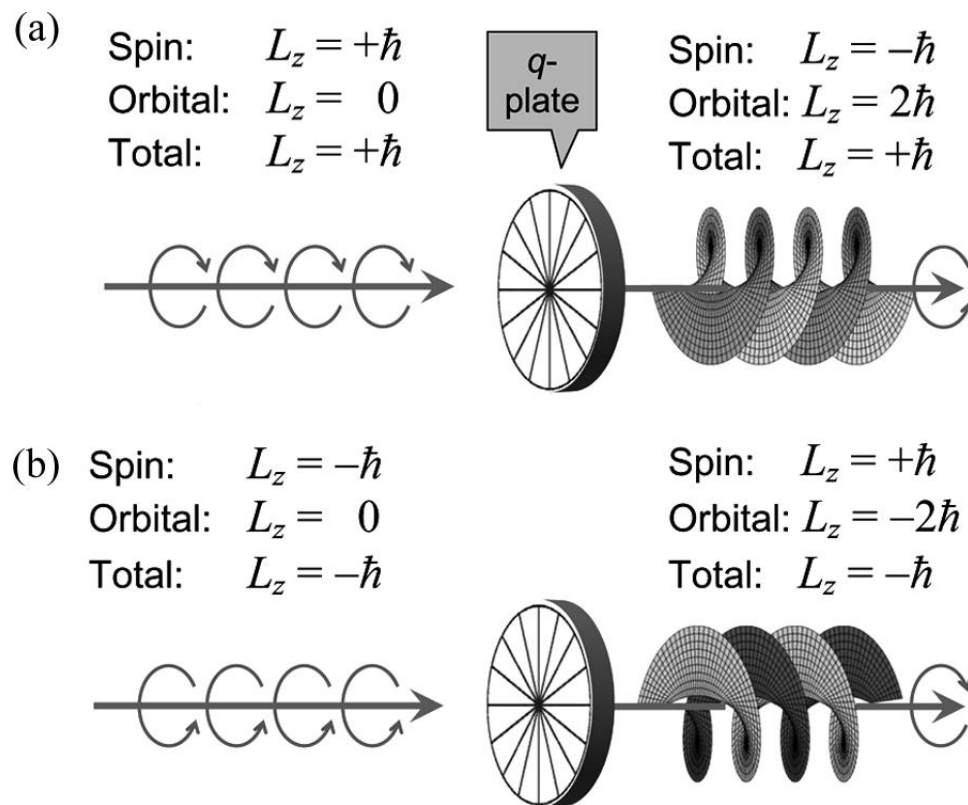
output: $L_{\text{spin}} = - \hbar$, $L_{\text{orbit}} = + 6\hbar$,

$L_z = L_{\text{spin}} + L_{\text{orbit}} = 5\hbar$ per photon

$L_z = L_{\text{spin}} + L_{\text{orbit}} = 5\hbar$ per photon

One example from another approaches to the same problem
here by application of liquid crystals forming a q-plate

Spin-to-orbital angular momentum conversion occurring for a single photon



(a) CL input polarization. (b) CR input polarization.

L. Marucci (2008)

Spin-to-orbit angular momentum XPC conversion

at conventional (dielectric and transparent) interfaces and multilayers
total angular momentum is conserved exactly

$$L_z = L_{\text{spin}} + L_{\text{orbital}} = \text{const.}$$

for each photon in the beam and for the whole beam field of cylindrical symmetry

however,

the vortex excitation and annihilation
induced at these structures are weak

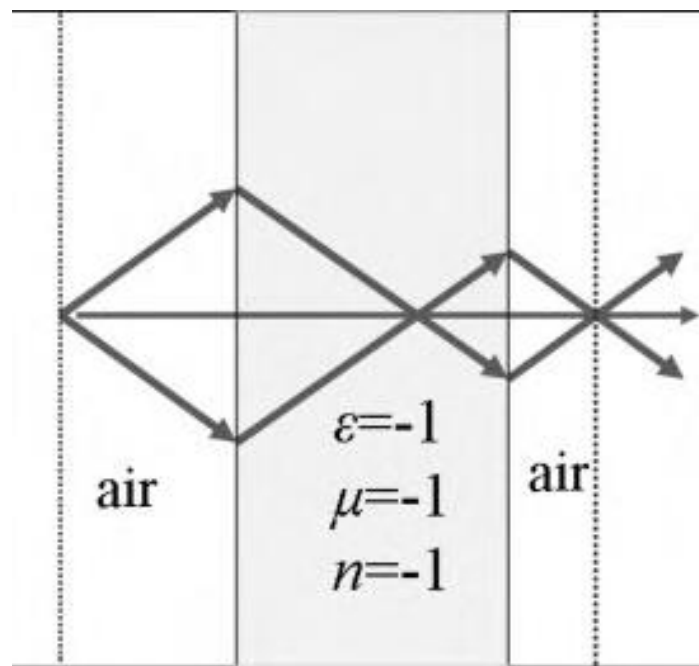
possible remedy may be based, for example, on application of:

- anisotropic media
- metamaterial media

further, one example of the second possibility will be shortly presented

Superlens action of a Double Negative (DNG) metamaterial layer

Metamaterials do not exist in nature and can only be fabricated artificially. In DNG ($\epsilon < 0$, $\mu < 0$, $n < 0$) metamaterials waves exhibit phase and energy velocities of opposite directions.

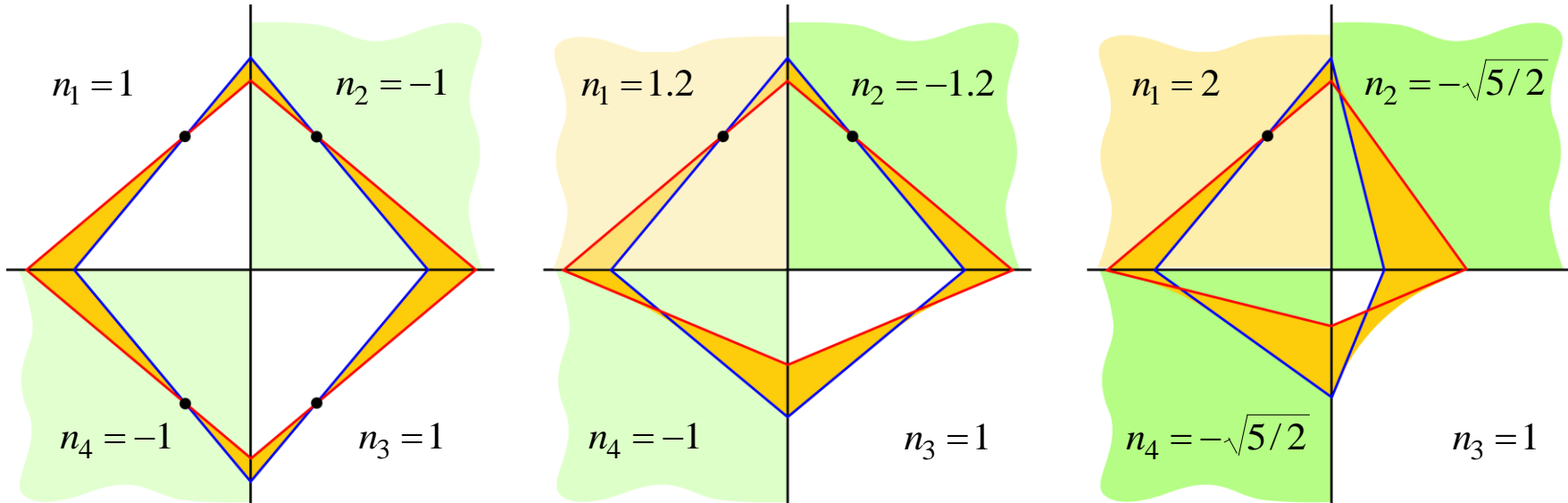


A DNG medium bends light to a negative angle relative to the surface normal. Light formerly diverging from a point in the object plane is reversed and converges back exactly to a point.

after: V. G. Veselago (1968), J. B. Pendry (2000), C. M. Soukoulis, et al (2006).

Resonator cavity build from lossless dielectrics and DNG metamaterials

due to the dielectric-metamaterial interfaces the cavity works without any mirror

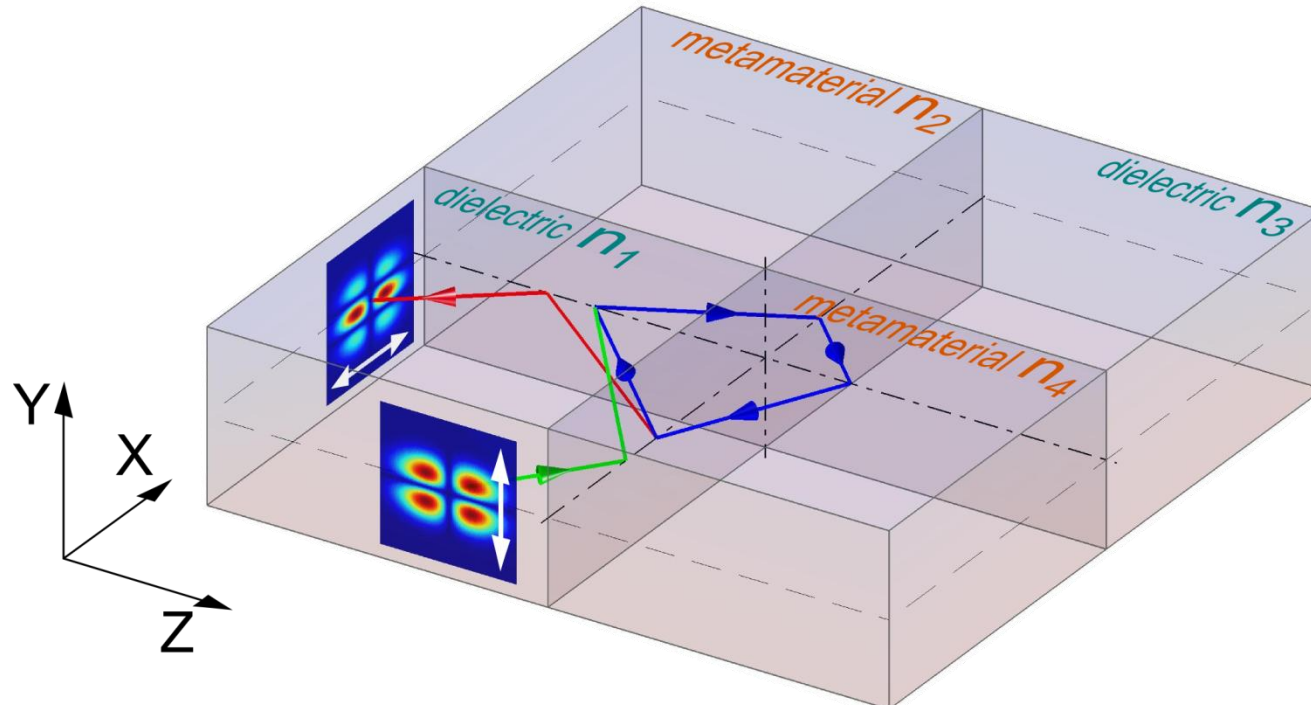


Three cavities provide ideal focusing of rays at least at one point in one space quadrant. The ideal foci are indicated by black dots. Impedance matching at the inter-media boundaries and a number of ideal focusing points differentiate the type of the cavity.

the third case, without any impedance matching, is chosen for numerical simulations

3D view of the nano-meta-resonator cavity

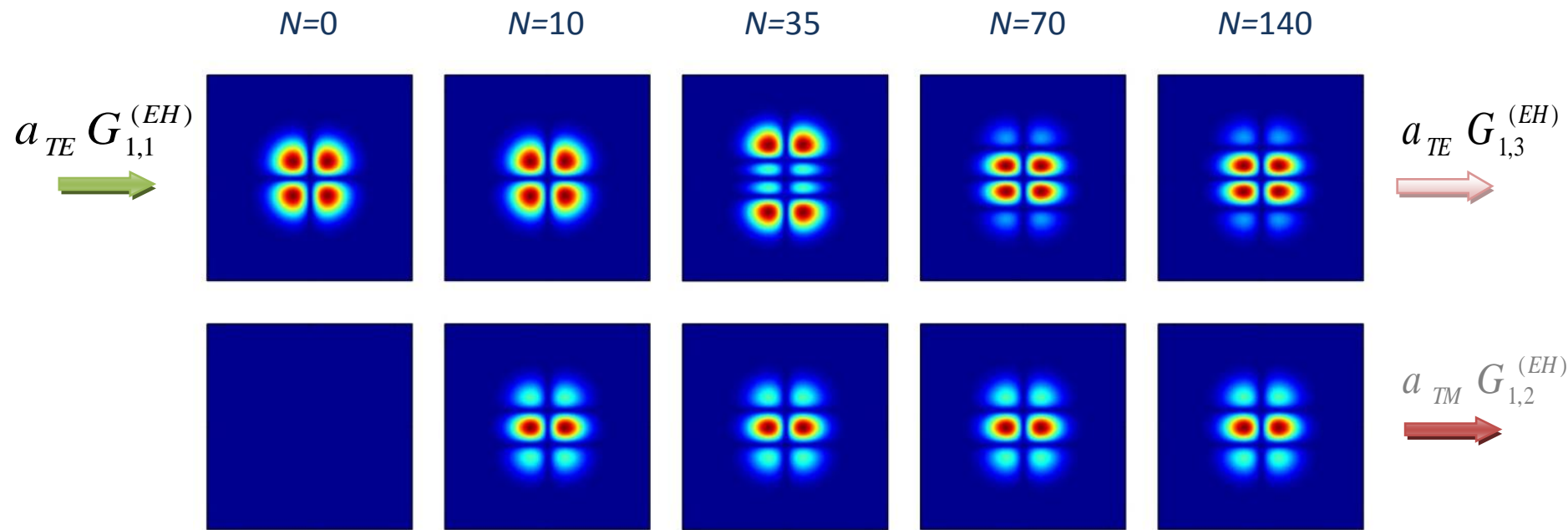
the beam polarization **TE-TM** and the beam spatial **EHG** shape switching occurs due to the cross-polarization coupling at the cavity interfaces under their collective resonant action



the incident beam is of $\text{EHG}_{1,1}$ transverse field shape,
the green line represents the coupling path of the beam of linear-vertical polarisation,
the blue line represents the propagation in the cavity,
the red line represents the decoupling path of the beam of linear-horizontal polarization.

Resonant enhancement of the cross-polarization coupling in the cavity

switching from the $\text{EHG}_{1,1}$ beam of TE polarization to the $\text{EHG}_{1,2}$ beam of TM polarization



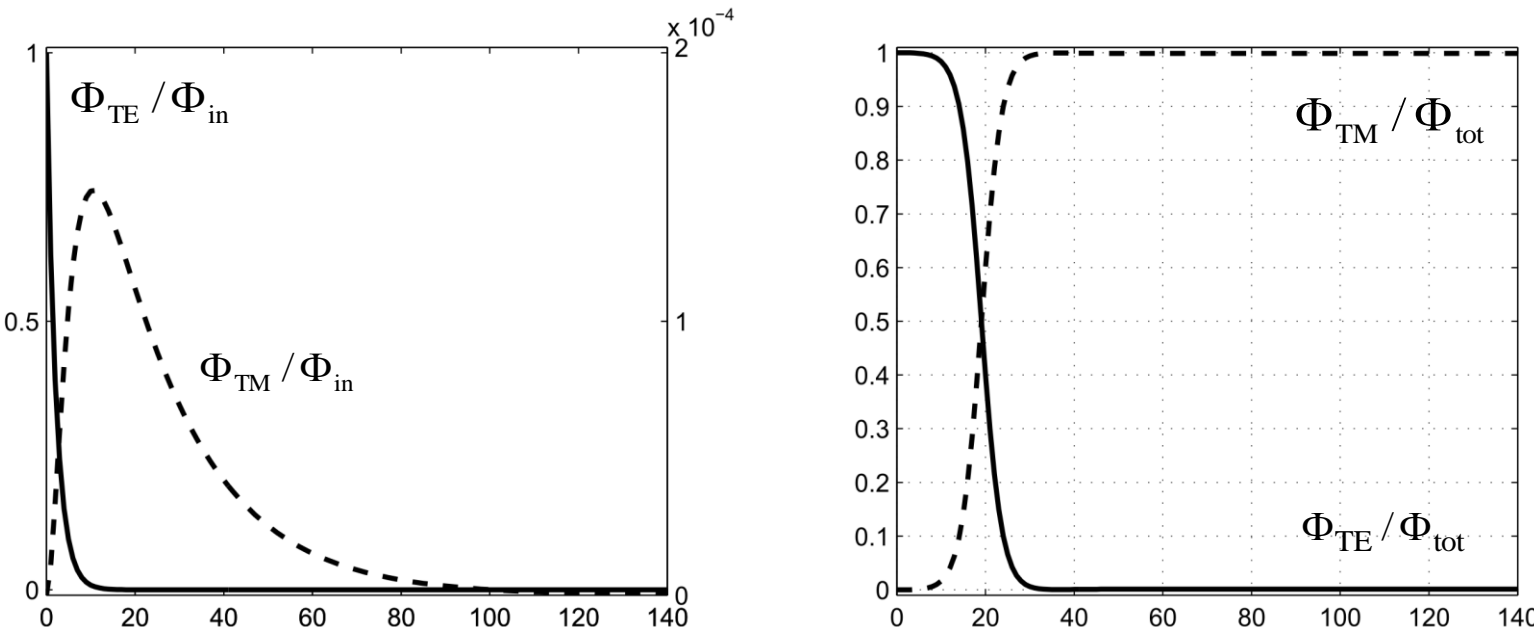
Beam amplitude decompositions in two orthogonal polarization components for the input TE beam polarization. Amplitudes of the TE polarization (the first row) and in the TM polarization (the second row) at the middle plane in medium 1 for $N = 0, 10, 35, 70, 140$ round trips.

WS & WN, J. Phys. B. At. Mol. Opt. Phys. (2011)

Rada Naukowa IPPT PAN, sesja sprawozdawcza 26.04.2012

TE – TM cross-polarization switching in the resonator cavity

the input beam of **TE** polarization switch to the output beam is of **TM** polarization



Contribution of beam polarization components to the total beam power after N th round trips in the resonator; scaled to the input beam power (a) and scaled to the propagating beam power (b).

figure (b) clearly confirms the 100% switch from TE polarization to TM polarization of the beam

WS & WN, J. Phys. B. At. Mol. Opt. Phys. (2011)

Rada Naukowa IPPT PAN, sesja sprawozdawcza 26.04.2012

Applications

qubit and qudit optical encoding
entanglement and hyperentanglement of photons and biphotons
quantum information - computing, cryptography and teleportation
super-resolution imaging, optical cloaking
and other sci-fi-like nano-meta-devices
nano trapping, manipulation and self-assembling
near-field nano-visualisation advances
to mention a few

other recent research topics conducted in the Research Group of Nanophotonics

near-field nano-visualisation
plasmonic applications in nano-photonics
nano-manipulation and nano-assembling by light

THANK YOU FOR ATTENTION